8th Power Electronics, Drive Systems & Technologies Conference (PEDSTC 2017)
14-16 Feb. 2017, Ferdowsi University of Mashhad, Mashhad, Iran

Robust Control of a DC-DC Boost Converter: H_2 and H_∞ Techniques

Yousef Khayat, *Student Member, IEEE*, Mobin Naderi, *Student Member, IEEE*, Qobad Shafiee, *Member, IEEE*, Yazdan Batmani, Mohammad Fathi , and Hassan Bevrani, *Senior Member, IEEE*

Smart/Micro Grids Research Center (SMGRC)
Department of Electrical and Computer Engineering, University of Kurdistan, Sanandaj, Iran
Y.khayat@eng.uok.ac.ir

***Abstract*-- This study proposes H_2 and H_∞ robust controllers to be applied to a DC-DC boost converter operates in the continuous conduction mode (CCM) in a DC microgrid system. Towards this end, the DC-DC boost converter is modelled based on the state-space averaging method with possible uncertainty in its parameters and also considerable variation in the input voltage. By deriving the open loop perturbed transfer function, an unstructured uncertainty bound for the nominal system is presented. Next, two robust controllers (i.e., H_2 and H_∞) are designed to regulate the DC bus voltage in the presence of drastically variations in the input voltage, the input inductor, the output capacitor, and the DC bus load. Simulation results demonstrate that the proposed controllers are strongly robust against uncertainties and can be applied to a practical DC microgrid.**

***Index Terms*—Boost converter, DC microgrids, H_2, H_∞ , robust control, uncertainty.**

I. Introduction

THE ADVENT of microgrids because of the increasing penetration of renewable energy resources (RESs) is becoming more and more. Due to some acute problems in AC microgrids such as synchronization of distributed generators (DGs), inrush current, and three-phase unbalance[1], [2], and also some essential advantages of DC microgrids, the solution of DC microgrids has become an attractive issue. Complete control of energy flow, no need for the synchronization of distributed generators, easily compensation of power fluctuation in DC bus by using energy storage devices with fast dynamics, and higher efficiency than AC microgrids are the impressive benefits of these networks[3]–[5].

DC-DC converters, such as boost type, buck type, and buck-boost type, have been widely used in DC microgrids as an interface between common DC bus, RES and energy storage system (ESS). Due to the intermittent nature of RESs like photovoltaic and wind energy, the generated power of these sources, and, accordingly their output voltage are variable and seriously affected by climatic condition, wind intensity, and the irradiation[6]–[9]. Thus, it is absolutely essential to have a DC-DC converter as an interface between RESs/ESSs and DC bus to provide a fixed output voltage. Among the different types of DC-DC converters, the boost converter is the most used interface stage in DC microgrids with archetypal efficiencies of 70-90% that generate a greater output voltage than its input voltage[10]–[12].

In comparison with the other DC-DC converters, buck or buck-boost converters, the bilinear dynamics and non-minimum phase characteristic of boost converter are a challenging control problem[10], [11]. This makes the control design of the boost converter more difficult especially in microgrid applications where common perturbations, e.g., voltage variation, can unstable the system [7], [9].

In the recent years, various control strategies for the DC-DC power converters with applications in microgrids have been applied [13]–[16]. Proper modeling of a system is essential to design an advanced controller. Unlike the methods which use fuzzy logic and neural networks, a proper model of a boost converter needs to describe the various aspects of the system behavior [17]. Therefore, many models have been proposed including: nonlinear autoregressive moving average with exogenous input (ARMAX) models procured by means of identification, Hammerstein models and small-signal models obtained by averaging techniques [18]–[20]. In [18], a specific linearized procedure is utilized around the operating point to approximate the nonlinear system, while the stability of the system could not be assured. Furthermore, linear control methods [11], sliding mode nonlinear controllers[14], [16], [20], classical digital control techniques [21], and robust internal model control according to the Hammerstein structure [22] have been recently introduced for such systems. Despite the work done in [20]–[22], it is not necessary to identify the parameters of a boost converter, since voltage stability, i.e., regulation of the DC bus voltage to a desired set point is the main objective in a DC microgrid. In [22] the selection of a static nonlinearity function always is a critical problem which affect the authenticity of the Hammerstein model which this will be the main issue of this control algorithm. Ref. [16] and [21] introduce an improved-equivalent control-based sliding mode controller for DC-DC converters. This control approach solves the problem of variable switching frequency and chattering phenomena and provides a fast dynamic in comparison with conventional ones but unsatisfactory robustness against system uncertainties.

To the best of our knowledge, there is no significant work done on robust control of DC-DC converters and DC microgrids using H_2 and H_∞. A robust H_2 controller has been introduced recently in [23], however, the robustness against parameter's uncertainty has not been taken into account.

This paper proposes a systematic procedure for designing robust controllers, H_2 and H_∞, for a DC-DC boost converter operating in continuous conduction mode (CCM). Multiplicative uncertainty of the system is considered and a

stable, minimum-phase transfer function to the upper-bound frequency responses is characterized. By representing the linear fractional transformation of the closed-loop system with lumped multiplicative uncertainties, control design procedure is reformulated as optimization problems which can be solved easily. In order to investigation of designed robust controllers several simulations including a Monte Carlo analysis as a comprehensive comparison for all uncertainties are stated.

The reminder of this paper is outlined below. In Section II, a detailed small-signal averaged model with parasitic resistors of the input inductor and the output capacitor is presented. Section III discusses about all possible uncertainties of a DC-DC boost converter. In Section IV, the robust control techniques are represented. Section V evaluates performance of these designed controllers on the DC-DC boost converter under different uncertainties. Finally concluding remarks are presented in Section VI.

II. Small Signal Average Model of Boost Converters

Boost converter which is a non-isolated step-up DC-DC converter, is the most frequent power electronic interface between RESs and local consumers in DC microgrids. To synthesis and design of a robust controller for such a system, LTI transfer function is required. Small signal averaged technique is one of the best that can be applied to a DC-DC converter. Simplicity of this technique can be the main reason to be applied to DC microgrids with DC-DC boost interfaced (with unidirectional or bidirectional structure).

The circuit framework of a boost converter is shown in Fig. 1, where v_{in} and v_o are the input and output voltages, respectively, S_1 is the MOSFET or IGBT power electronic switch, L, C, R_L and R_C are the input inductor, output capacitor filter, resistance of the input inductor and output capacitor, respectively. By using the circuit laws, differential equations to derivate state space equations can be represented as

$$\begin{cases} \dot{x} = A_1 x + B_1 u & S_1: ON \\ \dot{x} = A_2 x + B_2 u & S_2: OFF \end{cases}, \qquad (1)$$

where $x = \begin{bmatrix} i_L & v_c \end{bmatrix}^T$, $u = v_{in}$,

$$A_1 = \begin{bmatrix} -R_L/L & 0 \\ 0 & -1/C.(R_{Load}+R_C) \end{bmatrix}, \quad B_1 = \begin{bmatrix} 1/L \\ 0 \end{bmatrix},$$

$$A_2 = \begin{bmatrix} -R_L/L - 1/L.(R_{Load}\|R_C) & -R_{Load}/L.(R_{Load}+R_C) \\ R_{Load}/C.(R_{Load}+R_C) & -1/C.(R_{Load}+R_C) \end{bmatrix} \text{ and } B_2 = B_1.$$

In this case, the average model can be achieved as $\bar{\Lambda} = \Lambda_1.d + \Lambda_2.(1-d)$, where Λ represents state-space or input matrices and d is the static gain of DC-DC converter. In general designs, R_{Load}, L, C, v_{in} and therefore, d are often regarded as ideal constant. However, in DC-DC converter interfaced microgrids, all of them, specially v_{in}, and accordingly d, are not constant because of intermittent nature of input voltage; they should be considered as variables.

Given that all the parameters of the boost converter are known, the nominal state-space average model can be represented as follows

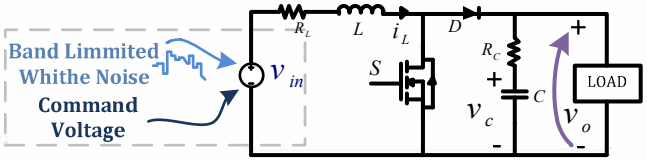

Fig. 1. Circuit model of a boost converter.

$$\bar{A} = \begin{bmatrix} -R_L/L - (1-d).(R_{Load}\|R_C)/L & -R_{Load}.(1-d)/L.(R_{Load}+R_C) \\ R_{Load}.(1-d)/C.(R_{Load}+R_C) & -1/C.(R_{Load}+R_C) \end{bmatrix}, \qquad (2)$$

and $\bar{B} = B_2 = B_1$.

It is obvious that once voltage drop on R_C is negligible, the output voltage will be equal with the v_c.

III. System Uncertainty Model

Due to intermittent nature of RESs, output power of these sources will be always along with some severe deviation which causes severe deviation in the load voltage. In this circumstances a robust controller is necessary. To design such a controller, a detailed model of the system along with possible uncertainties is necessary.

There are several definitions for modeling of a system with uncertain parameters in robust control theory [24]. In general, a system with uncertainty or dynamic perturbation can be mainly categorized into "un-modeled dynamics", and "modeling errors". In here, dynamic parametric perturbations considered for the boost DC-DC converter are lumped into perturbation of $\Delta_m(s)$ which is an unstructured uncertainty. In order to model unstructured uncertainty in robust control theory, several methods such as additive perturbation, inverse additive perturbation and input/output multiplicative perturbation have been introduced [24]. In this paper, the multiplicative perturbation method is used for uncertainty modeling. Thus, transfer function of the system in the presence of uncertainties can be formulated as

$$G_\Delta(s) = [1 + W_u(s).\Delta_m(s)]G_n(s), \quad \bar{\sigma}[\Delta(j\omega)] < 1, \quad \forall \omega \geq 0 \qquad (3)$$

where $W_u(s)$ is a stable scalar transfer function that characterize the frequency structure and spatial of the uncertainty, spans the $G_\Delta(s)$ to a neighborhood of the nominal model $G_n(s)$, and $\bar{\sigma}$ is the largest singular value of $\Delta_m(s)$. It should be noted that (3) does not imply any mechanism or structure for uncertain disk of $\Delta_m(s)$. The main uncertainties are caused by L, C, R_{Load} and especially v_{in}. The uncertainties radius are addressed in Table I.

Fig. 2 shows the bode diagram for the perturbed system for different values of the constant static gain. As it can be seen, negative phase margin of the transfer function demonstrates the non-minimum phase characteristic of (2).

To obtain an unstructured uncertainty bound for this system, by defining the multiplicative uncertainty $\Delta_m(s)$, a $W_u(s)$ can be found such that $|\Delta_m(j\omega)| \leq |W_u(j\omega)|$.

Thus, a $W_u(s)$ is given by

$$W_u(s)=\frac{1.2(s^2+43.1s+3.5\times10^4).(s^2+1467s+1.7\times10^6)}{(s^2+204.4s+2.9\times10^5).(s^2+665.8s+3.1\times10^6)} \quad (4)$$

IV. Robust H_2 and H_∞ Controller Design

Photovoltaic generation systems are the most conventional systems that produce a variance in the output voltage under variable irradiation and temperature, and also variable load conditions, resulting in serious control challenges. Therefore, a stable robust controlled DC-DC converter is necessary in order to employ the generation unit energy be more efficient. The aim of this section is to design an H_∞ and an H_2 robust voltage controllers for the system shown in Fig. 2. The robust controllers are applied using a feedback signal from the output voltage (see Fig. 3).

TABLE I. Nominal Value and Uncertainty Radius of Boost Converter

Parameter	Nominal value	Uncertainty radius
C	860 μF	$600\mu F \le C_n \le 1000\mu F$
L	860 μH	$600\mu H \le L_n \le 1000\mu H$
d	0.4	$0.3 \le d_n \le 0.5$
R_L	0.01 Ω	0
R_C	0.01 Ω	0

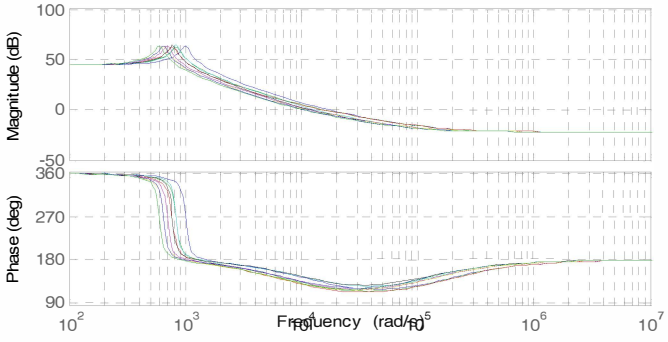

Fig. 2. Bode diagram of perturbed system for variation in duty cycle.

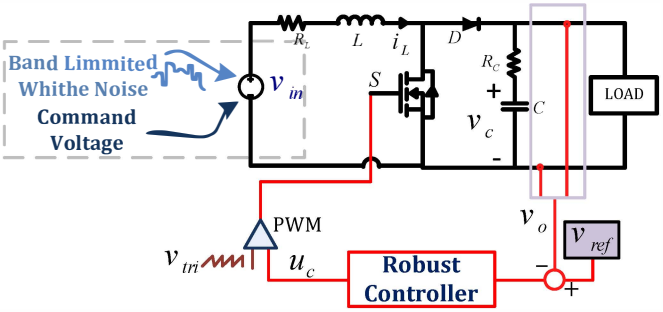

Fig. 3. General scheme of a robust controlled boost converter.

TABLE II. Optimization Problems Related to the Controllers Designs

Controller	Corresponded norm or cost function
H_2	$\|F_L(G,K)\|_2 < 1$
H_∞	$\|F_L(G,K)\|_\infty < 1$

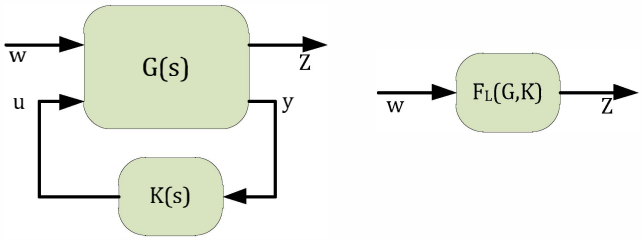

Fig. 4. Standard LFT configuration for design of the robust controllers.

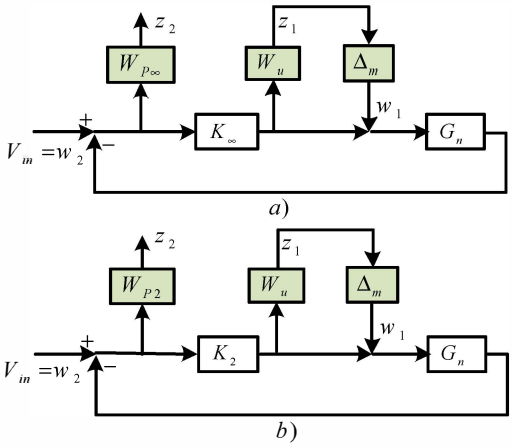

Fig. 5. Closed-loop system diagram to synthesis of robust controllers: (a) H_∞, (b) and H_2 .

It is noteworthy that in this study the control laws do not require the measurement of the current flowing into the inductor. The robust controllers' objective is achieved by minimizing the corresponding norms of an appropriate linear fractional transformation, $F_L(G,K)$, as depicted Table II. $F_L(G,K)$ is the transfer function matrix of the nominal closed-loop system which can be illustrated as transfer function T_{ZW} [24], as shown in Fig. 4. It must be noted that the solution for the corresponded minimization problems are not unique; it is generally adequate to find a stabilizing controller such that the corresponded norms of Table II go below one. By rewriting $F_L(G,K)$ as $z = T_{zw} w$ (see Figs. 5(a) and 5(b)), the closed-loop transfer function in matrix form is

$$\begin{bmatrix} z_1 \\ z_2 \end{bmatrix} = \begin{bmatrix} GK(1+GK)^{-1} & (1+GK)^{-1} \\ -G(1+GK(1+GK)^{-1}) & 1-G(1+GK)^{-1} \end{bmatrix} \begin{bmatrix} w_1 \\ w_2 \end{bmatrix}, \quad (5)$$

where, K is the corresponded designed controller based on H_∞ or , H_2. Similarly, the transfer function for mixed H_2/H_∞ is obtained as

$$\begin{bmatrix} z_1^\infty \\ z_2^2 \\ z_3^2 \end{bmatrix} = \begin{bmatrix} K(1+GK)^{-1} & GK(1+GK)^{-1} \\ K(1+GK)^{-1} & GK(1+GK)^{-1} \\ (1+GK(1+GK)^{-1}) & -G(1-GK(1+GK)^{-1}) \end{bmatrix} \begin{bmatrix} w_\infty \\ w_2 \end{bmatrix}. \quad (6)$$

For specification the H_∞ controller, it is shown that if $\|T_{ZW}\|_\infty < \gamma$, the system without any controller is robustly stable if and only if $\|\Delta_m\|_\infty \le 1/\gamma$ [24]. In general, for designing

the robust controllers it is tried to minimize the corresponded norms in Table II.

A. Robust H_∞ Controller

Fig. 5(a) shows the closed-loop system used for design of the robust H_∞ controller where $W_{P\infty}$ is the weighting function for obtaining the good tracking aims. This weighting function is chosen as

$$W_{P\infty}(s)=\frac{0.95s+82.5}{s+0.01}. \quad (7)$$

Note that the desirable performance of the system can be ensured by mixed sensitivity constraints, as

$$\left\| \begin{pmatrix} W_{P\infty}(s).S(s) \\ W_u(s)T(s) \end{pmatrix} \right\|_\infty < 1, \quad (8)$$

where $S(s)=(1+G(s)K(s))^{-1}$ and $T(s)=K(s)(1+G(s)K(s))^{-1}$ are the sensitivity functions. Therefore, the H_∞ problem can be reformulated by the following optimization problem.

$$\min_{K_\infty(s)} \left\| \begin{bmatrix} GK_\infty(1+GK_\infty)^{-1} & (1+GK_\infty)^{-1} \\ -G(1+GK_\infty(1+GK_\infty)^{-1}) & 1-G(1+GK_\infty)^{-1} \end{bmatrix} \right\|_\infty . \quad (9)$$

$$s.t \quad \left\| \begin{pmatrix} W_{P\infty}(s).S(s) \\ W_u(s)T(s) \end{pmatrix} \right\|_\infty < 1$$

B. Robust H_2 Controller

Following similar procedure as H_∞, H_2 controller is designed. As aforementioned, an important requirement to attain a successful design is the proper choice of the weighting function $W_{P2}(s)$. A proper selection of $W_{P2}(s)$ can be

$$W_{P2}(s)=\frac{s+10}{s^2+s+0.01}. \quad (10)$$

Accordingly, the controller is reformulated by the following optimization problem.

$$\min_{K_2(s)} \left\| \begin{bmatrix} GK_2(1+GK_2)^{-1} & (1+GK_2)^{-1} \\ -G(1+GK_2(1+GK_2)^{-1}) & 1-G(1+GK_2)^{-1} \end{bmatrix} \right\|_2 . \quad (11)$$

$$s.t \quad \left\| \begin{pmatrix} W_{P2}S \\ W_uT \end{pmatrix} \right\|_2 < 1$$

V. Simulation Results

In this section, the performance of the proposed control strategies is investigated under various scenarios. The DC-DC boost converter of Fig. 3 is implemented in the MATLAB/SimPowerSystems toolbox. A power supply which used to emulate a photovoltaic system taken as a power source with the nominal input voltage of $v_{in}=60$ V while a small variation (a random ±0.5 V) is mounted on it. Irradiation variations are modelled with a severe drop in input voltage. In the simulation studies frequent change of input voltage (by almost 15%) at t=0.3 s and t=0.6 s, is considered (see Fig. 6).

The effectiveness and robustness of the proposed controllers is verified under two sever case studies:

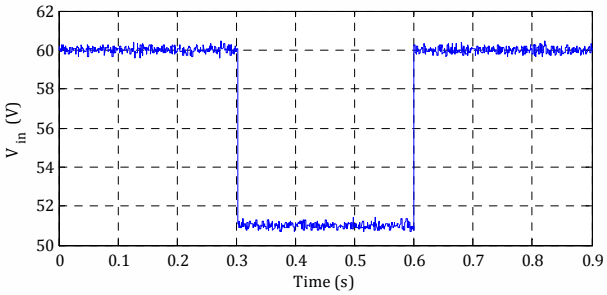

Fig. 6. Input voltage of the DC-DC boost converter for all cases.

Case 1: Robustness against 15% change in input voltage. The input voltage is reduced to $v_{in}=51$ V at t=0.3 s and goes back to the $v_{in}=60$ V at t=0.6 s while the DC bus load power is $P_{DC}=500$ W.

Case 2: 30% variation in the input inductor of L, output capacitor of C, are applied simultaneously with load increase and decrease as Monte Carlo analysis (a comprehensive analysis of DC-DC boost converter under input voltage variation, DC bus load changes, and parameters uncertainty of L and C).

Fig. 7(a) shows the performance of the designed robust controllers in regulating the DC voltage under input voltage variations. As can be seen the H_2 controller achieves a faster response in regulating DC voltage comparing the other one. High speed of the H_2 controller in regulation of DC link voltage refers to its inherent performance objectives of the H_2 optimal control problem. However, the lower voltage peak the H_∞ controller, when the input voltage changes, is because of robust performance and perturbation attenuation of this controller against system uncertainties. Fig. 7 shows the duty cycle of the DC-DC boost converter and the DC bus voltage. As shown, to regulate the output DC voltage on 100 V in the presence of input voltage variation, duty cycle increases 25%, approximately.

Figs. 8(a) and 8(b) indicate the load current and the inductor current. It is shown that the robust controllers provide satisfactory performance as variation of input voltage has a negligible effect on the load and inductor currents.

In the test condition number two, in addition to the above impacts, the impacts of load changes and parameter variations have been considered. For these purposes, there is 30% variation in parameters, moreover, at 0.4 second the load of the boost converter changes from 500 W to 250 W and at 0.7 second, it changes from 250 W to 1000 W (see Fig. 9), whereas still there are input voltage changes of the condition 1. Figs. 10(a) and 10(b) show the DC link output voltage and load current for this case, respectively.

At 0.3 second the impact of input voltage reduction, at 0.4 second, the impact of load reduction from 5 (500 W) to 2.5 A (250 W), at 0.6 second the impact of increasing of input voltage, and at 0.7 second the impact of increasing of the DC load from 2.5 A (250 W) to 10 A (1000 W) are completely obvious.

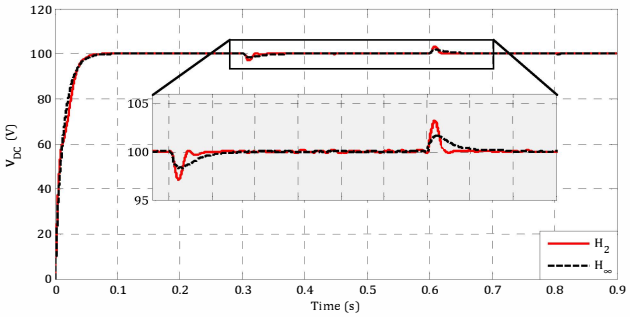

(a)

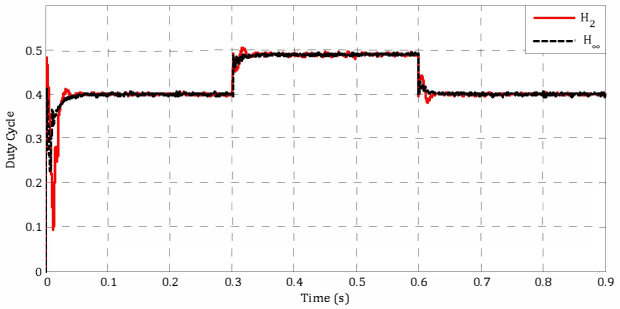

(b)

Fig. 7. Performance of the proposed robust controllers for study 1: (a) DC bus voltage, and (b) duty cycle.

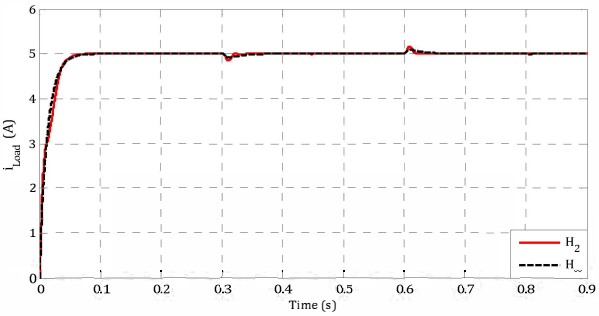

(a)

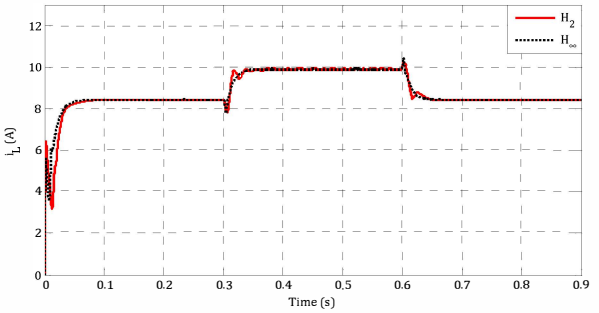

(b)

Fig. 8. Performance of the proposed robust controllers for study 1: (a) load current, and (b) inductor current.

Impressive performance of the proposed controllers in fixation of the DC bus is absolutely obvious. Fig. 9 shows the load current and the effects of voltage variations on it at 0.3 and 0.6 seconds.

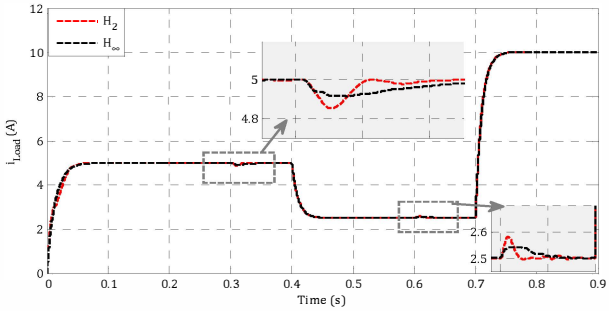

Fig. 9. Performance of the proposed robust controllers for load current changes

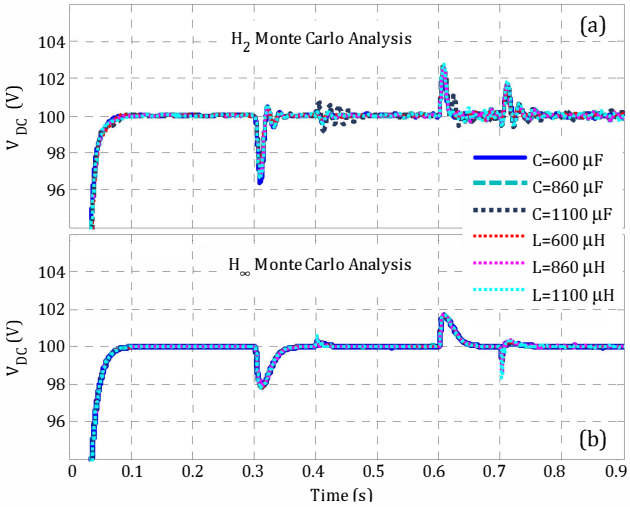

Fig. 10. Comprehensive robust performance analysis of the proposed controllers by Monte Carlo analysis for: (a) H_2, and (b) H_∞

Fig. 10 shows a comprehensive sensitivity analysis of the DC-DC boost converter under system uncertainties. Simulation studies are performed for all the robust controllers when $\pm 30\%$ variation in input inductor and output capacitor filter are considered in the presence of severe input voltage reduction and load disturbances. The results verify the robustness and excellent performance of the designed robust controllers. While simulation results related to H_2 show some variation in the DC bus voltage when a big load disturbance occur at $t= 0.7\ s$, the H_∞ controller shows more robustness against uncertainties. This controller retains its robustness and performance in simulations (which are not shown in here) for larger uncertainties in the mentioned parameters, i.e., 70% reduction and 200% increasing in inductor and capacitance variation.

VI. Conclusion

In this paper, two different robust controllers (H_2 and H_∞,) have been designed to set the output voltage of a DC-DC boost converter in the presence of various uncertainties. The robust performance of the obtained closed-loop systems have been evaluated by changing the input voltage of the DC-DC boost converter, the DC bus load, and $\pm 30\%$ variations in the input inductor and the output capacitor.

As it was expected, the H_2 controller has had the best performance especially when the input voltage and/or the DC

bus resistive load have changed. On the other hand, in the case of $\pm 30\%$ variations in the input inductor and the output capacitor, the H_2 controller has had the worst robustness property in comparison with the H_∞ controller. From a robust point of view, the H_∞ controller provided the best performance.

REFERENCES

[1] R. Lasseter, "Microgrids," *Eng. Soc. Winter Meet. 2002. IEEE*, 2002.

[2] H. Bevrani, *Robust Power System Frequency Control*, Second. Cham: Springer International Publishing, 2014.

[3] D. Wu, F. Tang, T. Dragicevic, J. M. Guerrero, and J. C. Vasquez, "Coordinated Control Based on Bus-Signaling and Virtual Inertia for DC Islanded Microgrids," *IEEE Trans. Smart Grid*, vol. 6, no. 6, pp. 1–12, 2015.

[4] A. P. N. Tahim, D. J. Pagano, E. Lenz, and V. Stramosk, "Modeling and Stability Analysis of Islanded DC Microgrids under Droop Control," *IEEE Trans. Power Electron.*, vol. 30, no. 8, pp. 4597–4607, 2015.

[5] M. Fathi and H. Bevrani, "Statistical cooperative power dispatching in interconnected microgrids," *IEEE Trans. Sustain. Energy*, vol. 4, no. 3, pp. 586–593, Jul. 2013.

[6] G. Adinolfi, G. Graditi, P. Siano, and A. Piccolo, "Multiobjective Optimal Design of Photovoltaic Synchronous Boost Converters Assessing Efficiency, Reliability, and Cost Savings," *IEEE Trans. Ind. Informatics*, vol. 11, no. 5, pp. 1038–1048, Oct. 2015.

[7] F. H. Aghdam and M. Abapour, "Reliability and Cost Analysis of Multistage Boost Converters Connected to PV Panels," *IEEE J. Photovoltaics*, vol. 6, no. 4, pp. 981–989, Jul. 2016.

[8] N. Eghtedarpour and E. Farjah, "Control strategy for distributed integration of photovoltaic and energy storage systems in DC micro-grids," *Renew. Energy*, vol. 45, pp. 96–110, 2012.

[9] C. Y. Hsieh, M. Moallem, and F. Golnaraghi, "A Bidirectional Boost Converter With Application to a Regenerative Suspension System," *IEEE Trans. Veh. Technol.*, vol. 65, no. 6, pp. 4301–4311, Jun. 2016.

[10] H. Liu, H. Hu, H. Wu, Y. Xing, and I. Batarseh, "Overview of High-Step-Up Coupled-Inductor Boost Converters," *IEEE J. Emerg. Sel. Top. Power Electron.*, vol. 4, no. 2, pp. 689–704, Jun. 2016.

[11] C. Basso, "DC-DC Converters Feedback and Control," *IEEE Appl. Power Electron. Conf. Expo. APEC*, 2009.

[12] A. Khosroshahi, M. Abapour, and M. Sabahi, "Reliability Evaluation of Conventional and Interleaved DC/DC Boost Converters," *IEEE Trans. Power Electron.*, vol. 30, no. 10, pp. 5821–5828, Oct. 2015.

[13] S. K. Kim and K. B. Lee, "Robust Feedback-Linearizing Output Voltage Regulator for DC/DC Boost Converter," *IEEE Trans. Ind. Electron.*, vol. 62, no. 11, pp. 7127–7135, Nov. 2015.

[14] S. Singh, D. Fulwani, and V. Kumar, "Robust sliding-mode control of dc/dc boost converter feeding a constant power load," *IET Power Electron.*, vol. 8, no. 7, pp. 1230–1237, Jul. 2015.

[15] A. K. Singha, S. Kapat, S. Banerjee, and J. Pal, "Nonlinear Analysis of Discretization Effects in a Digital Current Mode Controlled Boost Converter," *IEEE J. Emerg. Sel. Top. Circuits Syst.*, vol. 5, no. 3, pp. 336–344, Sep. 2015.

[16] E. K. Yaylaci and İ. Yazici, "Fast and robust voltage control of DC–DC boost converter by using fast terminal sliding mode controller," *IET Power Electron.*, vol. 9, no. 1, pp. 120–125, Jan. 2016.

[17] J. Han, D. Qiu, and B. Zhang, "Unified model of boost converter in continuous and discontinuous conduction modes," *IET Power Electron.*, vol. 9, no. 10, pp. 2036–2043, Aug. 2016.

[18] C. Y. Chan, "A Nonlinear Control for DC–DC Power Converters," *IEEE Trans. Power Electron.*, vol. 22, no. 1, pp. 216–222, Jan. 2007.

[19] M. Salimi and A. L. Eghlim, "Passivity-based control of the DC-DC buck converters in high-power applications," in *TENCON 2014 - 2014 IEEE Region 10 Conference*, 2014, pp. 1–6.

[20] R. S. Ashok and Y. B. Shtessel, "Sliding mode control of electric power system comprised of fuel cell and multiple-modular DC-DC boost converters," in *2014 13th International Workshop on Variable Structure Systems (VSS)*, 2014, pp. 1–7.

[21] G. Garcia, L. Martinez-Salamero, A. Marcos-Pastor, A. Cid-Pastor, and E. Vidal-Idiarte, "Discrete-time sliding-mode-based digital pulse width modulation control of a boost converter," *IET Power Electron.*, vol. 8, no. 5, pp. 708–714, May 2015.

[22] F. Alonge, F. D'Ippolito, and T. Cangemi, "Identification and robust control of DC/DC converter Hammerstein model," *IEEE Trans. power*, 2008.

[23] V. F. Montagner, L. a. Maccari, R. C. L. F. Oliveira, and H. Pinheiro, "Robust $\mathcal{H}2$ control applied to boost converters: design, experimental validation and performance analysis," *IET Control Theory Appl.*, vol. 6, no. 12, pp. 1881–1888, 2012.

[24] K. Zhou and J. C. Doyle, *Essentials Of Robust Control.* PRENTICE HALL, 1998.